Available online at www.sciencedirect.com

ScienceDirect

Journal of Magnesium and Alloys 1 (2013) 346−351
www.elsevier.com/journals/journal-of-magnesium-and-alloys/2213-9567

Full length article

Effect of Zr modification on solidification behavior and mechanical properties of Mg−Y−RE (WE54) alloy

Jilin Li, Rongshi Chen*, Yuequn Ma, Wei Ke

State Key Laboratory for Corrosion and Protection, Institute of Metal Research, Chinese Academy of Sciences, 62 Wencui Road, Shenyang 110016, China

Received 11 November 2013; revised 26 November 2013; accepted 3 December 2013

Abstract

Magnesium alloys containing rare earth elements (RE) have received considerable attention in recent years due to their high mechanical strength and good heat-resisting performance. Among them, Mg−5%Y−4%RE (WE54) magnesium alloy is a high strength sand casting magnesium alloy for use at temperatures up to 300 °C, which is of great interest to engineers in the aerospace industry. In the present work, the solidification behavior of Zr-containing WE54 alloy and Zr-free alloy was investigated by computer-aided cooling curve analysis (CA-CCA) technique. And the solidification microstructure and mechanical properties of them were also investigated comparatively. It is found from the cooling curves and as-cast microstructure of WE54 alloy that the nucleation temperature of α-Mg in WE54 alloy increases after Zr addition, and the as-cast microstructure of the alloy is significantly refined by Zr. While the phase constitution of WE54 alloy is not changed after Zr addition. These phenomena indicate that Zr acts as heterogeneous nuclei during the solidification of WE54 alloy. Due to refined microstructure, the mechanical properties of Zr-containing WE54 alloy is much higher than Zr-free WE54 alloy.
Copyright 2013, National Engineering Research Center for Magnesium Alloys of China, Chongqing University. Production and hosting by Elsevier B.V. Open access under CC BY-NC-ND license.

Keywords: WE54 alloy; Zr modification; Solidification behavior; Mechanical properties

1. Introduction

Magnesium alloys have the advantageous properties such as low density, high specific strength, good castability, and excellent machinability. And rare earth elements have been used as alloying elements to improve the mechanical properties of magnesium alloys since the 1920s. While the application of Mg−RE alloys have been obsessed by the coarse microstructure of these alloys until Sauerwald et al. found the grain-refining effect of zirconium on Mg−RE alloys such as Mg−Th alloy [1] and Mg−Ce alloy [2] in 1940s. It was found that the grain size of Mg−RE alloys were refined from millimeter scale to about 50 μm by Zr addition under normal cooling rate [3].

In recent years, magnesium alloys containing heavy rare earth elements (HRE) such as Gd, Y, Nd have received considerable attention due to their high mechanical strength and good heat-resisting performance [4−7]. Among them, Mg−5%Y−4%HRE−Zr (WE54) magnesium alloy is a high strength sand casting magnesium alloy, whose high temperature mechanical strength is the top of existing commercial magnesium alloys [8−10]. As a powerful grain-refiner in these alloys, zirconium is broadly believed to improve the mechanical property and corrosion resistance of these alloys [11], and lots of work have been carried out on the grain refining mechanism of Zr in magnesium alloys [12−14]. While these works were mainly carried out in Mg−Zr alloys, which are quite different in solidification behavior and microstructure

* Corresponding author.
E-mail addresses: jlli@imr.ac.cn (J. Li), rschen@imr.ac.cn (R. Chen), yqma@imr.ac.cn (Y. Ma), wke@imr.ac.cn (W. Ke).
Peer review under responsibility of National Engineering Research Center for Magnesium Alloys of China, Chongqing University

Production and hosting by Elsevier

2213-9567 Copyright 2013, National Engineering Research Center for Magnesium Alloys of China, Chongqing University. Production and hosting by Elsevier B.V. Open access under CC BY-NC-ND license.
http://dx.doi.org/10.1016/j.jma.2013.12.001

with Mg−RE−Zr alloys. So far, no detailed research has been carried out on exactly how Zr addition affects the solidification behavior and mechanical properties of these alloys to the author's knowledge, and the influence mechanism of Zr on solidification microstructure and mechanical properties of these alloys remain unclear.

In the present research, the solidification behavior of Zr-free and Zr-containing WE54 alloy were investigated by a computer aided cooling curve analysis (CA-CCA) technology and microstructure observation in order to study the effects of Zr addition on the solidification behavior of WE54 alloy. And the mechanical properties of Zr-free and Zr-containing WE54 alloy were studied comparatively, aiming at revealing the influence mechanism of Zr on solidification microstructure and mechanical properties of WE54 alloy.

2. Experimental procedures

2.1. Alloy casting and heat treatment

WE54 alloys with and without Zr addition were prepared from high purity Mg (99.95%), Gd (99%), Y (99%), Nd (99%) and/or Mg−30Zr (wt.%) master alloy by melting them in an electric resistance furnace under protection of an anti-oxidizing flux. The melt was poured into a steel mold preheated to 300 °C at about 780 °C to cast the alloy ingots. The actual chemical composition of the alloy was determined by using inductively coupled plasma atomic emission spectroscopy (ICP) and listed in Table 1. The solution treatment of the alloys was carried out at 525 °C for 6 h followed by water quenching, and the subsequent aging treatment was carried out at 250 °C for 16 h followed by air cooling.

2.2. Cooling curve analysis

Computer aided cooling curve analysis (CA-CCA) of the investigated alloys was performed by remelting and solidifying cylindrical samples of the alloys in a cylindrical graphite crucible placed in an electrical resistance furnace. The cylindrical samples with dimensions of Φ 30 mm × 60 mm were cut from the casting ingots using an electric discharge wire cutting machine, and burnished by sandpaper before remelting. After holding at 740−750 °C for 5 min, the graphite crucible was removed from the furnace, and the melt in the crucible began to solidify at a cooling rate of approximately 1 K/sec. During the melt solidification, the temperature variations of the melt were recorded continuously with a high speed data acquisition system at an acquisition frequency of 20 Hz. Then the temperature data were imported into Origin 8.5 data analysis software, and the cooling curve and its first derivative curve were calculated with this software in order to determine the characteristic features of the alloy solidification. In order to ensure reproducibility of the testing results, each test was carried out at least twice.

Table 1
Chemical composition of the experimental alloy (wt.%).

Element	Y	Nd	Gd	Zr	Mg
Zr-containing WE54 alloy	5.02	1.92	2.13	0.45	Balance
Zr-free WE54 alloy	5.10	1.91	2.03	−	Balance

2.3. Microstructure observation and tensile testing

Microstructure observations were conducted using optical microscope (OM) and scanning electron microscope (SEM) equipped with an energy disperse spectroscopy (EDS). Electron backscattered diffraction technology (EBSD) was used to measure the grain size of the investigated alloys. Samples for optical microscopy were etched in a solution of 4 vol.% HNO_3 in ethanol after mechanical polishing to reveal grain boundaries, no chemical etching was applied to specimens for SEM investigations, and the EBSD samples were electrochemical polished after grinding with sandpapers. The mean grain size, d, was determined by the linear intercept method using the equation $d = 1.74\,L$, where L is the linear intercept grain size determined by analyzing the EBSD micrographs of the investigated alloys.

The tensile tests of the WE54 alloys with and without Zr content at different heat treatment states were performed on standard round tensile specimens with the gauge length of 25 mm and the gauge diameter of 4 mm. Tensile test was conducted at room temperature with an initial strain rate of 10^{-3}/s on a universal testing machine. Three specimens were tested for each test condition to ensure the reliability of data. And the fracture morphology of the alloys was observed by SEM.

3. Results and discussion

3.1. Solidification behavior

Fig. 1 shows the thermal analysis results for the investigated alloys and their microstructures in the as-cast condition. It is seen from the cooling curves and the first derivative curves of the alloys that Zr-free and Zr-containing WE54 alloys experiences similar phase transformations during their solidification procedure. Thus the as-cast microstructure and phase constitution of Zr-free and Zr-containing WE54 alloys are similar as shown in Fig. 1(b) and (d). While the α-Mg phase nucleated at 637.5 °C in Zr-free WE54 alloy, which was lower than the nucleation temperature of 646 °C in Zr-containing WE54 alloy, as seen clearly on first derivative curves. So a higher supercooling degree is necessary for α-Mg nucleation in Zr-free WE54 alloy than in Zr-containing WE54 alloy, indicating that a transformation of nucleation mode occurs after Zr addition in WE54 alloy.

Fig. 2 shows the as-cast microstructure of WE54 alloy obtained by OM and EBSD techniques. It is found from the EBSD images shown in Fig. 2(a) and (c) that the as-cast microstructure of WE54 alloy is significantly refined after Zr addition. By linear intercept method, the average grain size of Zr-free and Zr-containing WE54 alloy is determined to be 295 μm and 83 μm, respectively. And the OM images show

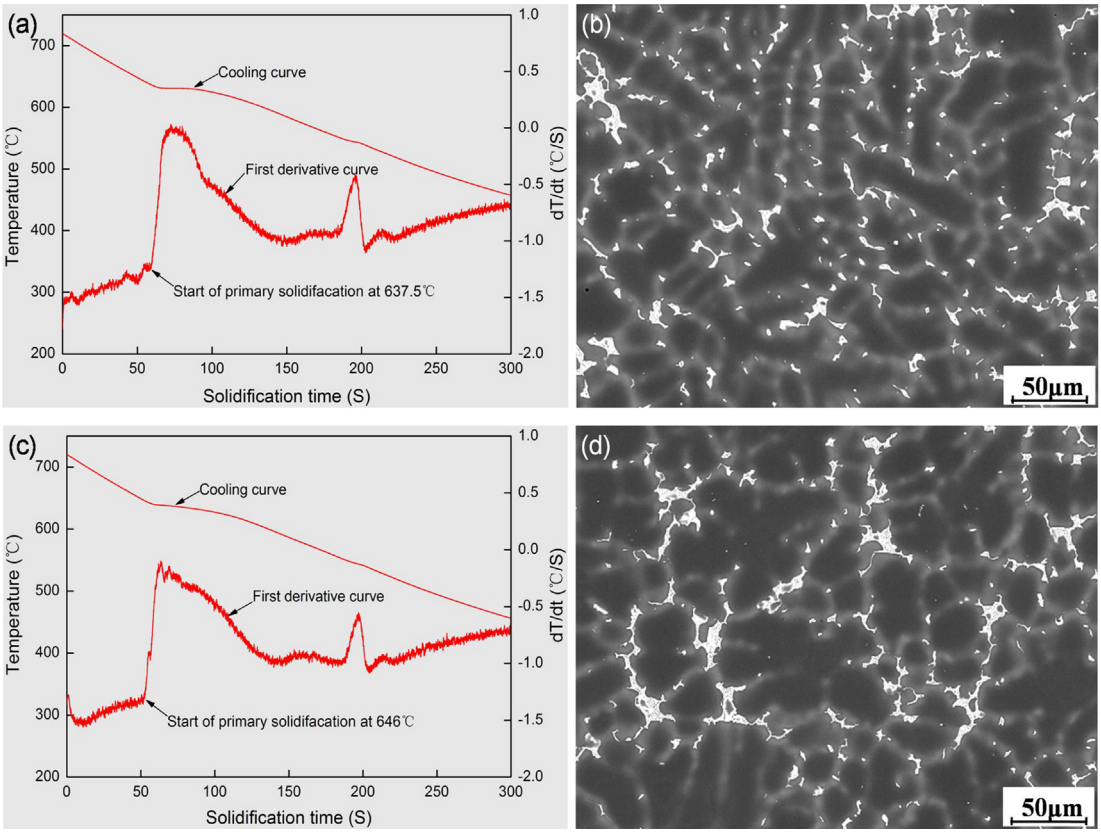

Fig. 1. Thermal analysis results and as-cast microstructures of the investigated alloys: (a) and (b) Zr-free WE54 alloy, (c) and (d) Zr-containing WE54 alloy.

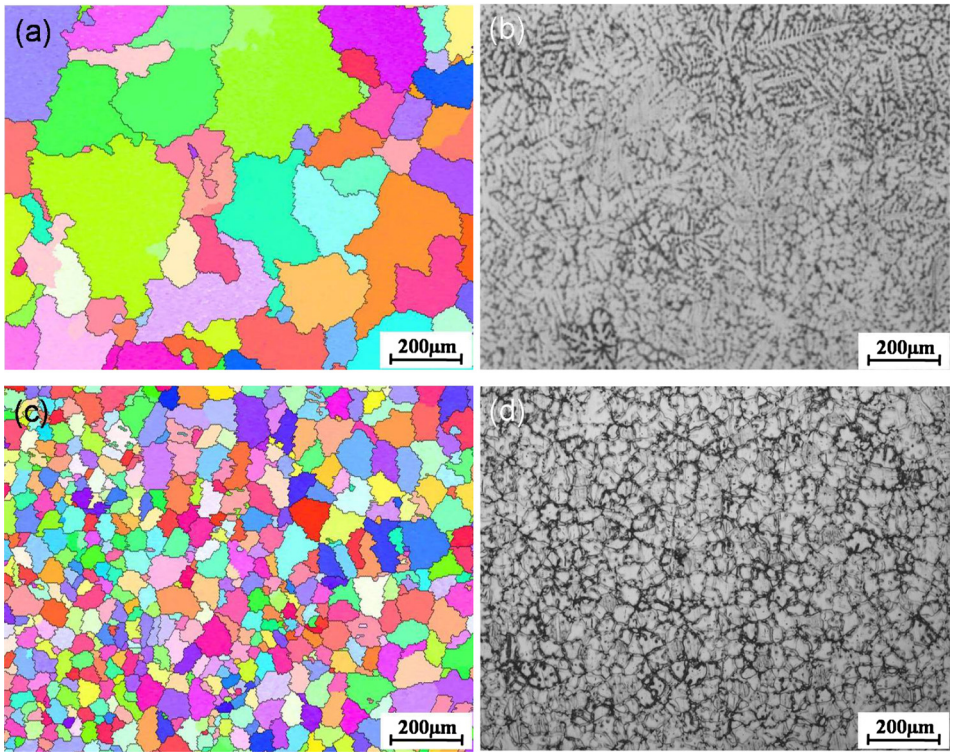

Fig. 2. As-cast microstructure of WE54 alloy obtained from OM and EBSD: (a) and (b) Zr-free WE54 alloy, (c) and (d) Zr-containing WE54 alloy.

that the microstructure of Zr-free WE54 alloy is composed of coarse, heterogeneous dendrites, while the microstructure of Zr-containing WE54 alloy is composed of fine and uniform equiaxed grains. Thus the microstructure of WE54 alloy is significantly refined by Zr addition, and the grain morphologies of WE54 alloy are modified by Zr addition as well.

Although the microstructure and the phase constitution of WE54 alloy are not affected by Zr addition. Some differences were detected through detailed observation of the as-cast microstructure by SEM. Fig. 3(a) shows the backscattered electron image of Zr-containing WE54 alloy. It is clear from the image that there are some white particles with a size of about 1 μm in the α-Mg matrix of the alloy microstructure. These particles are determined to be Zr-rich particles according to EDX composition analysis results shown in Fig. 3(b). This observation result coincides with the results of Lin et al. [15]. So the reason for the refinement effect of Zr on WE54 alloy microstructure is supposed to lie on these Zr-rich particles dispersed in α-Mg matrix.

Since Zr does not affect the phase constitution of WE54 alloy, it is believed that Zr is not involved in phase transformation reactions during the alloy solidification, which is in accordance with the Mg–Zr phase diagram shown in Fig. 4. As shown in Fig. 4, more than 0.565 wt.% Zr can be dissolved in Mg melt at temperatures higher than 650 °C. Thus a significant amount of Zr is dissolved in Mg melt during smelting of Zr-containing magnesium alloys, with respect to the smelting temperature of above 750 °C for Mg–RE alloys. When the melt is poured into casting molds, it solidifies at a relatively high cooling rate. When the temperature of the melt decreases to 650 °C, the dissolved Zr element precipitates uniformly from the melt and forms evenly distributed α-Zr particles in the melt. As mentioned in previous studies, zirconium and magnesium have the same type of crystal structure and almost identical lattice constants, which make the α-Zr particles perfect nucleating agents in magnesium alloys that are not alloyed with aluminum [12,14]. Thus the subsequently precipitated α-Mg phase nucleates on these α-Zr particles at 646 °C, and results in fine equiaxed grains in the as-cast microstructure of Zr-containing WE54 alloy. While the α-Mg phase nucleates homogeneously in Zr-free WE54 alloy, which need higher nuclear driving force and results in less nucleating agents. So the microstructure of Zr-free WE54 alloy was composed of coarse dendrites.

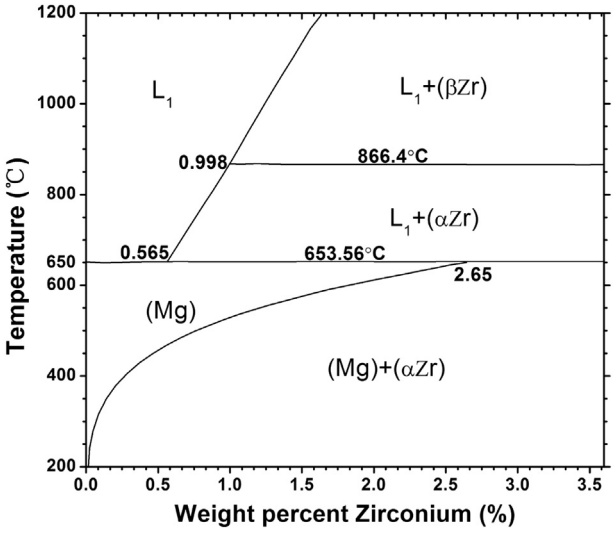

Fig. 4. Mg-rich region of the Mg–Zr phase diagram [16].

3.2. Mechanical properties

The tensile properties of Zr-free and Zr-containing WE54 alloy at different heat treatment conditions are displayed in Fig. 6 and Table 2. Compared to the as-cast alloys, significant solution strengthening and age hardening effects are observed in both Zr-free and Zr-containing WE54 alloys. The aged Zr-containing WE54 alloy displays the ultimate tensile strength

Table 2
Mechanical properties of Zr-free WE54 alloy and Zr-containing WE54 alloy.

Temper	Zr-free WE54 alloy			Zr-containing WE54 alloy		
	UTS [MPa]	YS [MPa]	EL [%]	UTS [MPa]	YS [MPa]	EL [%]
As-cast	173	146.7	1.0	211.7	149.7	5.1
Solution-treated	200	148	4.8	223	153.5	12.5
Peak-aged	242.5	222	0.8	274.5	194	8.2

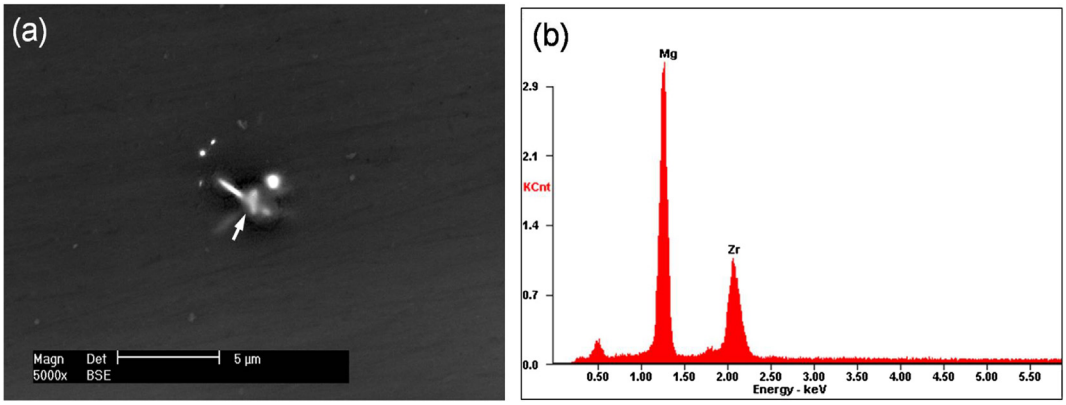

Fig. 3. Zr-rich particles observed in Zr-containing WE54 alloy.

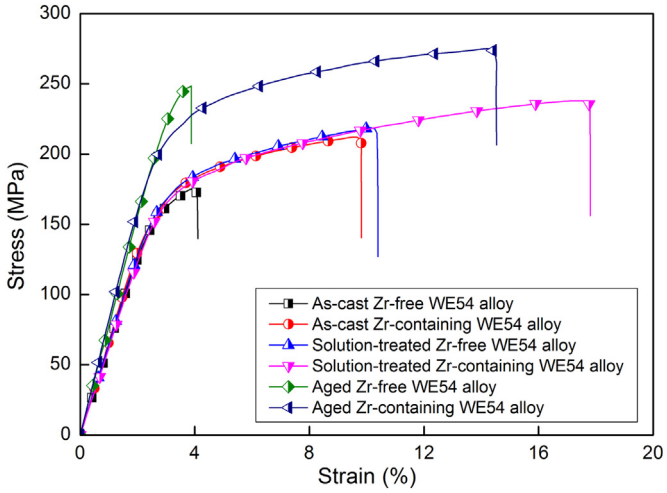

Fig. 5. Typical tensile curves of WE54 alloy with and without Zr addition.

(UTS) of 274.5 MPa and the tensile yield strength of 194 MPa, comparing with the UTS of 242.5 MPa and TYS of 222 MPa of aged Zr-free WE54 alloy. It is also found that the elongation rate of Zr-free WE54 alloy are significantly lower than that of Zr-containing WE54 alloy, due to refined microstructure of Zr-containing WE54 alloy.

Fig. 6 presents the fracture morphologies of the investigated Zr-free and Zr-containing WE54 alloys. Comparing these fracture morphologies, it is found that the fracture morphology changed markedly with heat treatment states in both Zr-free and Zr-containing WE54 alloys. Fig. 6a and b shows the fracture surfaces of the as-cast alloys, in which many broken eutectics are present in both Zr-free and Zr-containing WE54 alloys. As shown in Fig. 1, the eutectics are complex in shape with large aspect ratios, and they are prone to fracture at local stress concentrations during tensile test [17], so the microcracks form easily by the fracture of eutectic compounds in as-cast alloys. Hence, the as-cast alloys have the lowest tensile strength as seen in Fig. 5 and Table 2.

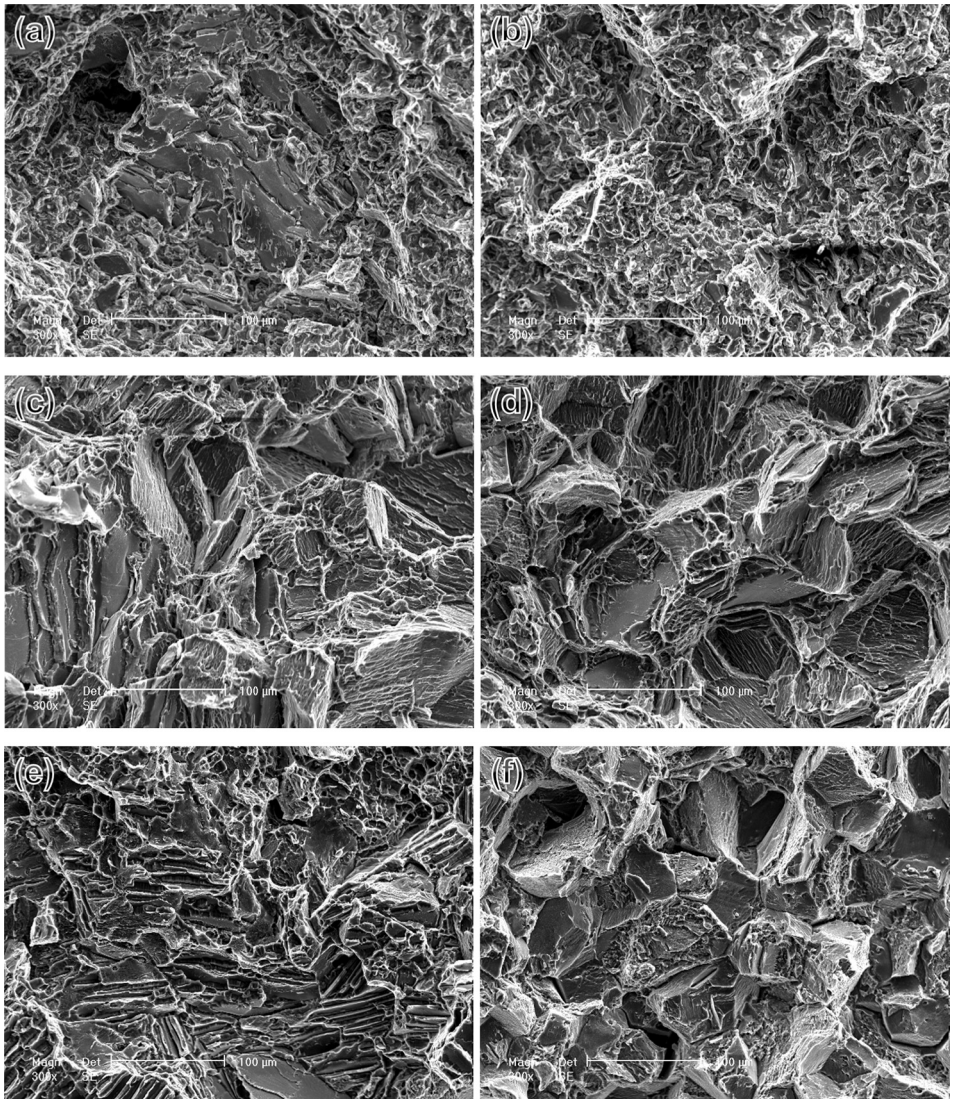

Fig. 6. Tensile fracture microstructures of the investigated alloys: (a) as-cast Zr-free WE54 alloy, (b) as-cast Zr-containing WE54 alloy, (c) solution-treated Zr-free WE54 alloy, (d) solution-treated Zr-containing WE54 alloy, (e) aged Zr-free WE54 alloy, (f) aged Zr-containing WE54 alloy.

Fig. 6c and d are the fracture surface images of the samples after solution treatment at 525 °C for 6 h, which present ductile fracture features with many dimples and tearing ridges. Accordingly, the solution-treated alloys show higher elongation rate compared to as-cast alloys. After aging at 250 °C for 16 h, the fracture mode of the alloys changes to entire transgranular cleavage, as shown in Fig. 6e and f. And many secondary cracks are visible on the fracture surface.

Although the fracture features of Zr-free and Zr-containing WE54 alloys are similar, some differences exist between them. In the as-cast state, some large cleavage planes are seen on fracture surface of Zr-free WE54 alloy, as shown in Fig. 6a, while no such fracture feature is found on fracture surface of Zr-containing WE54 alloy shown in Fig. 6b. And the fracture morphologies of Zr-free WE54 alloy are more heterogeneous compared to fracture morphologies of Zr-containing WE54 alloy. This is caused by deformation inhomogeneity of Zr-free WE54 alloy during a tensile test. And the coarse, heterogeneous microstructure of Zr-free WE54 alloy is the fundamental cause of its deformation inhomogeneity.

4. Conclusions

The solidification behavior of Zr-free and Zr-containing WE54 alloy was investigated by a computer aided cooling curve analysis (CA-CCA) technology and the mechanical properties of Zr-free and Zr-containing WE54 alloy were studied comparatively. As the alloy melt solidifies, the dissolved Zr element precipitates uniformly from the melt and forms evenly distributed α-Zr particles, which are perfect nucleating agents for subsequently precipitated α-Mg phase. So the heterogeneous nucleation procedure of WE54 alloy is promoted and its microstructure is significantly refined. Due to fine and uniform microstructure, both the tensile strength and elongation rate of Zr-containing WE54 alloy are much higher compared to that of Zr-free WE54 alloy.

Acknowledgments

This work was funded by the National Basic Research Program of China (973 Program) through project No. 2013CB632202.

References

[1] W.P. Saunders, F.P. Strieter, AFS. Trans. 60 (1952) 581.
[2] A.J. Murphy, R.J.M. Payne, J. Inst. Met. 73 (1946) 105.
[3] M. Sun, G.H. Wu, J.C. Dai, S. Pang, W.J. Ding, Foundry 59 (2010) 255 (in Chinese).
[4] I.A. Anyanwu, S. Kamado, Y. Kojima, Mater. Trans. 42 (2001) 1206.
[5] I.A. Anyanwu, S. Kamado, Y. Kojima, Mater. Trans. 42 (2001) 1212.
[6] G.H. Wu, Y. Zhang, W.C. Liu, W.J. Ding, J. Magnes. Alloys 1 (2013) 39.
[7] X. Li, W. Qi, K. Zheng, N. Zhou, J. Magnes. Alloys 1 (2013) 54.
[8] J.F. Nie, B.C. Muddle, Scr. Mater. 40 (1999) 1089.
[9] J. Wang, J. Meng, D.P. Zhang, D.X. Tang, Mater. Sci. Eng. A 456 (2007) 78.
[10] S.M. He, X.Q. Zeng, L.M. Peng, X. Gao, J.F. Nie, W.J. Ding, J. Alloys Compd. 427 (2007) 316.
[11] M. Sun, G.H. Wu, W. Wang, W.J. Ding, Mater. Sci. Eng. A 523 (2009) 145.
[12] Q. Ma, D.H. Stjohn, Int. J. Cast. Met. Res. 22 (2009) 256.
[13] Q. Ma, A. Das, Scr. Mater. 54 (2006) 881.
[14] Q. Ma, D.H. St John, M.T. Frost, Scr. Mater. 50 (2004) 1115.
[15] G.B. Lin, Z.D. Wang, Z. Zhong, L.F. Liu, Adv. Mater. Res. 142 (2011) 99.
[16] H. Okamoto, J. Phase Equilib. Diffus. 28 (2007) 305.
[17] L. Gao, R.S. Chen, E.H. Han, J. Mater. Sci. 44 (2009) 4443.